**Journal of Medical and Health Studies**
ISSN: 2710-1452
DOI: 10.32996/jmhs
Journal Homepage: al-kindipublisher.com/index.php/jmhs/index

# Biophysical characterization and antibacterial activity of green-synthesized silver nanoparticles from pomegranate (Punica granatum) peel extract against multidrug-resistant clinical isolates

**Ferial Y. Nazal**

*Department of Medical Physics and Physiology, College of Medicine, University of Thi-Qar, Nasiriyah, Iraq.*

**Corresponding Author:** Ferial Y. Nazal**, E-mail:** ferial-y@utq.edu.iq

## ABSTRACT

For several common infections, the spread of multidrug-resistant (MDR) bacteria has narrowed the range of usable antibiotics. Silver nanoparticles (AgNPs) are one candidate replacement, and making them with plant extracts keeps both the cost and the use of toxic reagents low. We set out to make AgNPs with pomegranate peel extract, describe their properties, and see how well they act on MDR isolates from patients and how toxic they are to Vero cells. An aqueous peel extract, with no other reducing agent, was added to 1 mM silver nitrate. The resulting particles were characterized using UV–visible and FTIR spectroscopy, X-ray diffraction, transmission electron microscopy, dynamic light scattering and zeta-potential measurement. Five patient isolates were tested by agar well diffusion, broth microdilution (MIC/MBC) and time-kill experiments; Vero cell toxicity was measured by MTT. SPR peak at 425 nm, almost unchanged after 30 days at 4 °C. FTIR band shifts (phenolic O–H, C=O) implicated extract polyphenols in reduction and capping. TEM: spherical particles, 22.5 ± 6.1 nm; DLS: 38.6 nm, PDI 0.21; zeta potential −28.4 mV. The lowest MIC (8 µg/mL) was recorded for Escherichia coli and the highest (32 µg/mL) for both methicillin-resistant Staphylococcus aureus (MRSA) and Klebsiella pneumoniae. At 2× MIC, viable counts dropped by 3 $\log_{10}$ within 8 h (E. coli) and 12 h (MRSA). The Vero $IC_{50}$ was 112.4 µg/mL (selectivity index 3.5–14.1). The peel-derived AgNPs were bactericidal against MDR isolates at concentrations under the Vero $IC_{50}$. Topical rather than systemic use looks like the most realistic application.

## KEYWORDS

silver nanoparticles; green synthesis; Punica granatum; antimicrobial resistance; MIC; cytotoxicity

## ARTICLE INFORMATION

**ACCEPTED:** 01 October 2026 **PUBLISHED:** 01 November 2026 **DOI:** 10.32996/jmhs.2026.7.11.5

## 1. Introduction

Few problems in medicine are as pressing as antimicrobial resistance (AMR). In 2019 alone, bacterial resistance is estimated to have directly caused 1.27 million deaths and to have been involved in 4.95 million deaths in total [1]. The WHO names several pathogens for which new treatments are urgently needed, including Enterobacterales that no longer respond to carbapenems or to cephalosporins of the third generation, and methicillin-resistant Staphylococcus aureus (MRSA) [2, 3]. Because many such strains are multidrug-resistant (MDR), the choice of effective antibiotics at the bedside is often narrow.

Only a handful of new antibiotic classes have reached the clinic in recent decades, so attention has turned to other antimicrobials. Silver is one of the oldest. It served as an antiseptic for centuries, and interest came back once it could be made as nanoparticles (AgNPs, 1–100 nm), mostly because at this scale the surface area per unit volume is huge and the metal becomes far more reactive [4, 5]. Some wound dressings, catheter coatings and device surfaces already carry AgNPs [5, 6], and they inhibit Gram-positive as well as Gram-negative bacteria [7].

AgNPs hit bacteria in more than one way at the same time. Particles that stick to the cell envelope may get through it and leave the membrane leaky [8, 9]. $Ag^+$ released from the surface binds the sulfhydryl groups of enzymes, upsetting respiration and DNA replication [10, 11], and the reactive oxygen species the particles generate damage proteins, lipids and nucleic acids [12]. Much of the toxicity comes from dissolved $Ag^+$. How quickly the metal dissolves depends on particle size, shape and coating [13–15], which is why smaller particles, with more surface per gram, are usually more active [15]. The spectrum of AgNPs covers Gram-negative and Gram-positive bacteria and extends to yeasts [16], and their activity is retained against antibiotic-resistant strains [17]. Bacteria

**Copyright:** © 2026 the Author(s). This article is an open access article distributed under the terms and conditions of the Creative Commons Attribution (CC-BY) 4.0 license (https://creativecommons.org/licenses/by/4.0/). Published by Al-Kindi Centre for Research and Development, London, United Kingdom.

are not defenceless, though. With repeated exposure, strains that make flagellin can emerge; this protein makes the particles aggregate, and once aggregated they no longer work [18]. For this reason, any new AgNP preparation should be both thoroughly characterized and tested with standardized antimicrobial methods [19]. Chemical routes to AgNPs typically rely on harsh reductants such as sodium borohydride, and physical routes consume considerable energy [20]. Plant-mediated synthesis is simpler and cheaper and avoids hazardous reagents [20–22]. In such extracts, polyphenols, flavonoids, terpenoids and proteins first convert $Ag^{+}$ to $Ag^{0}$ and then bind to the new particles, forming a coating that keeps them apart [21, 22]. After AgNPs were first made with neem leaf broth [23], the approach was extended to extracts of a large number of other plants.

The peel accounts for much of the weight of the pomegranate (Punica granatum L.) and is normally thrown away. It contains large amounts of hydrolysable tannins, notably punicalagin and ellagic acid, together with flavonoids and phenolic acids [24], which makes it a natural candidate for reducing and stabilizing silver. Pomegranate peel AgNPs have been prepared before, but mainly for catalysis [25]. Less is known about how such particles perform against carefully characterized MDR isolates from patients, and how toxic they are to mammalian cells at the same concentrations. In this study, AgNPs were prepared with an aqueous peel extract and their optical, chemical, structural and colloidal properties were measured. Their activity against MDR clinical isolates was then tested by diffusion and dilution methods, the speed of killing was followed with time-kill curves, and toxicity to a mammalian cell line was measured to estimate selectivity.

## 2. Materials and methods

### *2.1 Chemicals and plant material*

Silver nitrate (purity ≥ 99.0%), dimethyl sulfoxide (DMSO) and MTT were supplied by Sigma-Aldrich; Mueller–Hinton agar and broth were Oxoid products. Fresh pomegranates were purchased in November 2025 from a Nasiriyah market. After botanical identification, a voucher specimen was lodged in our department at the College of Medicine, University of Thi-Qar. All laboratory work was done at the same college.

### *2.2 Preparation of pomegranate peel extract*

Fruits were peeled by hand. The peels were washed (distilled water, three times), shade-dried at room temperature for 7 days and ground. The powder (10 g) was boiled in deionized water (100 mL) for 15 min, left to cool, passed through Whatman No. 1 paper and centrifuged (5,000 × g, 10 min) to remove fine debris. It was stored at 4 °C, and no batch was used after more than a week.

### *2.3 Synthesis of silver nanoparticles*

Ten millilitres of extract were dripped slowly into 90 mL of 1 mM $AgNO_3$ kept at 60 °C on a magnetic stirrer, so that the final $Ag^{+}$ level was 0.9 mM. The flask was wrapped in aluminium foil for the whole reaction to avoid light-induced reduction of silver. Progress was followed by eye from the colour of the mixture and by UV–visible scans taken at 0, 15, 30, 60 and 120 min. At 2 h the product was pelleted (12,000 × g, 20 min). Three wash cycles in deionized water removed unbound extract, after which the pellet was freeze-dried. For every experiment a fresh 1 mg/mL suspension was made in sterile water and bath-sonicated (10 min).

### *2.4 Characterization*

- **UV–visible spectroscopy:** a double-beam spectrophotometer ([manufacturer, model, country]) recorded 300–700 nm at 1 nm steps [26]. The sample was re-measured after 30 days in the refrigerator (4 °C) as a stability check.
- **FTIR:** KBr pellets of the dry extract and of the dry AgNPs were scanned from 4,000 to 400 $cm^{-1}$ ([manufacturer, model, country]); comparing the two spectra showed which groups had reacted with silver.
- **XRD:** the powder was scanned from 20° to 80° (2θ) on a diffractometer ([manufacturer, model, country]) fitted with a copper anode (Kα, 1.5406 Å). Crystallite size was calculated from the broadening of the (111) peak [27].
- **TEM:** diluted suspension was deposited on carbon-coated grids, left to dry in air and examined at 200 kV ([manufacturer, model, country]). At least 200 particles per sample were sized in ImageJ.
- **DLS and zeta potential:** hydrodynamic diameter, PDI and zeta potential were read three times per sample on a Malvern Zetasizer ([model]; Malvern Panalytical, UK), with the cell held at 25 °C [28, 29].

The Scherrer equation was applied in the form

$$D = K\lambda / (\beta \cos \theta)$$

in which D denotes crystallite size, K the shape constant (0.9), λ the Cu Kα wavelength, β the full width at half maximum of the (111) reflection (in radians) and θ the Bragg angle.

### *2.5 Bacterial isolates*

Five clinical isolates (MRSA, MSSA, Escherichia coli, Klebsiella pneumoniae and Pseudomonas aeruginosa, one of each) came from the microbiology laboratory at Al-Nasiriyah Teaching Hospital, and we rechecked identification and antibiograms on a VITEK 2 system (bioMérieux, France). MDR status followed the usual definition, i.e. non-susceptibility to ≥ 1 drug in ≥ 3 classes [30]. E. coli ATCC 25922 and S. aureus ATCC 29213 were run alongside as reference strains.

### 2.6 Agar well diffusion assay

Suspensions adjusted to 0.5 McFarland (≈ 1.5 × $10^8$ CFU/mL) were swabbed evenly over Mueller–Hinton agar plates [31]. Wells 6 mm across were cut in the agar, and each got 100 µL of AgNPs at 100 µg/mL. Controls were gentamicin (10 µg/mL), water, plain extract, and $AgNO_3$ at an equivalent silver content. Zones were read after 24 h at 37 °C.

### 2.7 MIC and MBC

We followed CLSI M07 for broth microdilution [32, 33]. Doubling dilutions of AgNPs (256 → 1 µg/mL) were set up in 96-well plates and inoculated to give 5 × $10^5$ CFU/mL per well. Plates were read after 18–20 h at 37 °C; the first well without turbidity gave the MIC. For the MBC, 10 µL aliquots from every well without visible growth were plated on agar; the MBC was taken as the smallest concentration that allowed no more than 0.1% of the starting inoculum to survive.

### 2.8 Time-kill assay

E. coli and MRSA were chosen for time-kill testing (CLSI M26-A) [34]. Each was exposed at about 5 × $10^5$ CFU/mL to 1× and 2× MIC of AgNPs; one tube had no AgNPs. Viable counts were determined at 0, 2, 4, 8, 12 and 24 h by plating serial ten-fold dilutions (detection limit 2 $\log_{10}$ CFU/mL). We counted a ≥ 3 $\log_{10}$ drop from the starting count as bactericidal.

### 2.9 Cytotoxicity assay

Vero cells (African green monkey kidney; [source and catalogue no., e.g. ATCC CCL-81]) were grown in Dulbecco's modified Eagle medium with 10% fetal bovine serum in a humidified incubator (37 °C, 5% $CO_2$). Cells were plated at $10^4$ per well, allowed one day to adhere, and then given AgNPs (6.25 to 200 µg/mL) for 24 h. MTT (0.5 mg/mL) was then added for 4 h, and the resulting formazan crystals were solubilized in DMSO before absorbance was measured at 570 nm [35]. Results are given as percent viability relative to untreated control wells. We fitted the dose–response data by nonlinear regression to get the $IC_{50}$ and divided it by the MIC to obtain the selectivity index (SI).

### 2.10 Statistical analysis

All values are reported as mean ± SD from three separate experiments. For each isolate the AgNP zone was compared with the gentamicin zone by unpaired t-test in GraphPad Prism 10, with $P < 0.05$ taken as significant.

## 3. Results

### 3.1 Synthesis and UV–visible spectroscopy

Within 15 min of adding the extract, the pale yellow $AgNO_3$ solution had turned reddish brown; at 30 min it was dark brown. The darkening reflects surface plasmon resonance (SPR) excitation in newly formed silver particles and therefore signals reduction of $Ag^+$ to $Ag^0$. An SPR peak was already visible in the 15 min scan. It kept rising until 60 min and then stayed constant, so we took the reaction to be finished by then. The 120 min spectrum had a single peak at 425 nm (Figure 1), typical of small silver spheres [26]. A month later (4 °C) the peak sat at 427 nm and had lost only 6% of its height; there was no sign of aggregation. Each 100 mL batch (0.9 mM $Ag^+$) contained 9.7 mg of silver, which is the upper limit for the metallic yield of one batch.

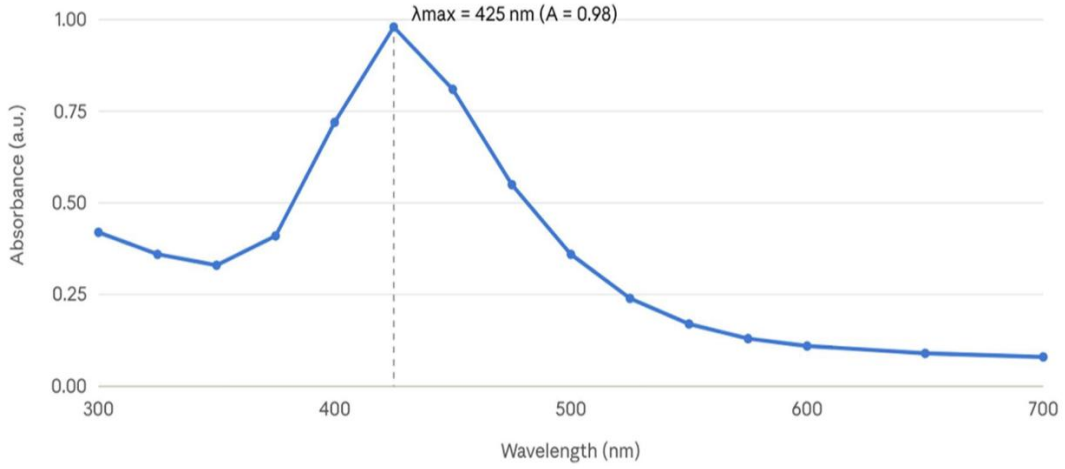


Figure 1. Absorption spectrum of the pomegranate-peel AgNP colloid, recorded over 300–700 nm 120 min after the extract was added to $AgNO_3$. Dashed line: SPR maximum (425 nm).

### 3.2 FTIR analysis

The main extract bands were still present in the AgNP spectrum, though several were shifted and less intense (Table 1). Shifts were largest for O–H and C=O stretching. Our reading is that phenolic hydroxyls were oxidized while donating electrons to $Ag^+$, and the oxidized polyphenols and tannins then remained bound to the metal surface.

Table 1. Main FTIR bands of the peel extract and of the AgNPs.

| Assignment | Extract ($cm^{-1}$) | AgNPs ($cm^{-1}$) |
|---|---|---|
| O–H stretching (phenols) | 3,412 | 3,385 |
| C–H stretching (aliphatic) | 2,925 | 2,921 |
| C=O stretching (ester of ellagitannins) | 1,718 | 1,704 |
| C=C stretching (aromatic ring) | 1,612 | 1,628 |
| O–H bending (phenols) | 1,342 | 1,350 |
| C–O stretching (alcohols, esters) | 1,038 | 1,031 |

### *3.3 Structural and colloidal characterization*

Four reflections appeared in the diffractogram, at 2θ = 38.1°, 44.3°, 64.4° and 77.4°; these index to the (111), (200), (220) and (311) planes of fcc silver (JCPDS 04-0783). We saw no $Ag_2O$ or AgCl peaks, so the product was pure metallic silver. TEM showed mostly spherical, separate particles of 9–41 nm (Table 2).

Table 2. Physicochemical properties of the AgNPs (mean ± SD, n = 3).

| Property | Method | Value |
|---|---|---|
| SPR peak | UV–visible | 425 nm |
| Crystallite size | XRD (Scherrer) | 18.7 nm |
| Core particle size | TEM (n = 200 particles) | 22.5 ± 6.1 nm |
| Hydrodynamic diameter | DLS | 38.6 ± 4.2 nm |
| Polydispersity index | DLS | 0.21 ± 0.03 |
| Zeta potential | Electrophoretic mobility | −28.4 ± 1.9 mV |

The XRD crystallite size (18.7 nm) and the TEM diameter (22.5 nm) were not far apart, so we think most particles are single crystals. DLS gave a larger figure than TEM. That was expected, since DLS measures the silver core together with the hydrated layer of biomolecules on it. A PDI of 0.21 means the sizes were fairly uniform [29], and at −28.4 mV, past the usual −25 mV cut-off, the particles repel each other enough to stay dispersed [28].

### *3.4 Antibacterial activity*

All five isolates were inhibited (Table 3). Escherichia coli needed the least silver (MIC 8 µg/mL), whereas methicillin-resistant Staphylococcus aureus (MRSA) and Klebsiella pneumoniae needed the most (MIC 32 µg/mL). MBC values were uniformly double the MIC (MBC/MIC = 2), pointing to a killing rather than a merely inhibitory effect. No zones formed around wells containing water or extract alone, and silver nitrate at the same silver content gave only narrow zones (8–10 mm).

Table 3. Activity of AgNPs against the clinical isolates. Zone diameters (mean ± SD, n = 3; the 6 mm well is included) were obtained with 100 µg/mL AgNPs.

| Isolate | Resistance profile | AgNP zone (mm) | Gentamicin zone (mm) | MIC (µg/mL) | MBC (µg/mL) |
|---|---|---|---|---|---|
| E. coli | ESBL-producing, MDR | 19.8 ± 0.9 | 9.3 ± 0.4 | 8 | 16 |
| P. aeruginosa | MDR | 17.1 ± 0.6 | 15.6 ± 0.7 | 16 | 32 |
| MSSA | Susceptible | 16.4 ± 0.8 | 22.1 ± 0.6 | 16 | 32 |
| MRSA | MDR | 13.2 ± 0.7 | 11.0 ± 0.5 | 32 | 64 |
| K. pneumoniae | Carbapenem-resistant, MDR | 12.6 ± 0.8 | No zone | 32 | 64 |

AgNP zones were wider than gentamicin zones for all four MDR isolates ($P < 0.05$). MSSA was the exception: here gentamicin did better ($P < 0.05$). Because the AgNPs were loaded at ten times the gentamicin concentration (100 vs. 10 µg/mL), these comparisons only describe this assay format, not true relative potency.

### *3.5 Time-kill kinetics*

Untreated cultures of both organisms increased by over 3 $\log_{10}$ CFU/mL in 24 h (Figure 2). With 2× MIC, E. coli fell by 3.5 $\log_{10}$ CFU/mL by the 8 h sample and was undetectable at 12 h, whereas MRSA took until 12 h to drop by 3 $\log_{10}$. At the MIC itself, counts of both organisms fell steadily, yet neither reached the 3-log threshold by 24 h. The rate of killing thus increased with concentration and was higher for the Gram-negative organism.

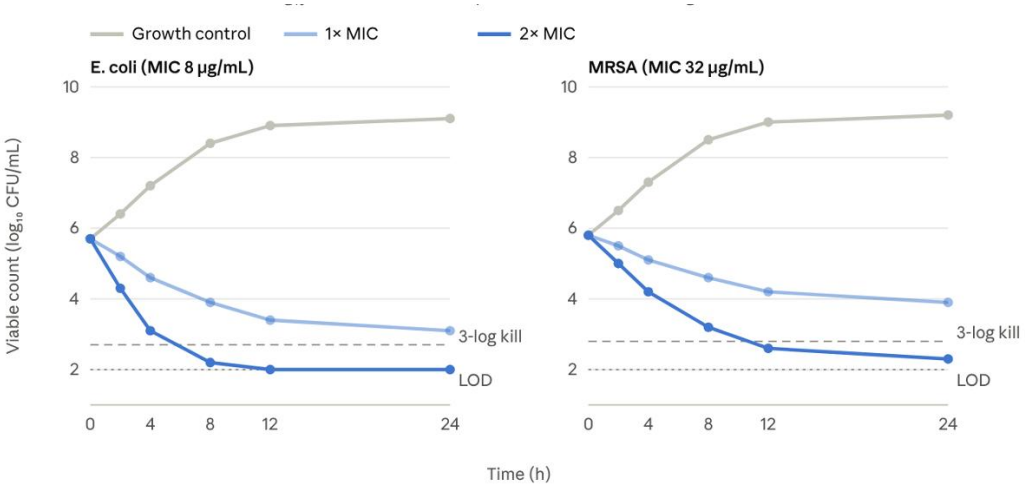


Figure 2. Killing curves for E. coli (left panel) and MRSA (right panel) exposed to AgNPs at the MIC and at twice the MIC, with an untreated control for comparison. Each point is the mean count from three replicates. The dashed line shows the bactericidal threshold (3-$\log_{10}$ decrease from the starting count), and the dotted line marks the detection limit (2 $\log_{10}$ CFU/mL).

### *3.6 Cytotoxicity and selectivity*

Vero viability declined with dose, giving an $IC_{50}$ of 112.4 µg/mL (Figure 3). At 32 µg/mL, our highest MIC, 87% or more of the cells were still alive. Selectivity indices ($IC_{50}$/MIC) were 14.1 for E. coli, 7.0 for both P. aeruginosa and MSSA, and 3.5 for both MRSA and K. pneumoniae.

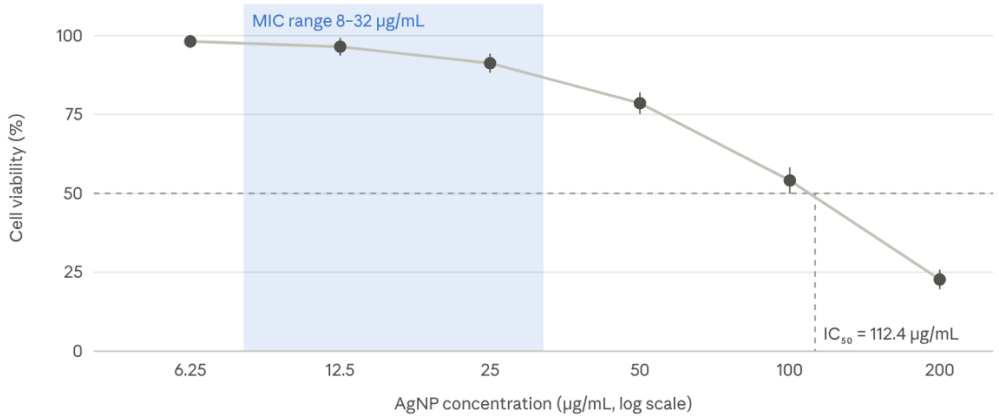


Figure 3. Viability of Vero cells (MTT assay) after a 24 h exposure to AgNPs over 6.25–200 µg/mL; points are means ± SD of three replicates. The shaded band covers the range of MICs for the tested isolates (8–32 µg/mL); dashed lines indicate 50% viability and the $IC_{50}$ (112.4 µg/mL).

## 4. Discussion

In this work the water extract of pomegranate peel was both the reductant and the stabilizer, and nothing else had to be added. What came out were small, stable silver crystals that killed MDR hospital isolates at doses Vero cells tolerated reasonably well.

Synthesis and characterization. Together, the SPR band at 425 nm, the fcc diffraction pattern and a mean TEM diameter of approximately 22 nm confirm the formation of metallic silver nanoparticles [21, 26]. A narrow plasmon band at this position is what Mie theory gives for silver spheres of about this size [26], and the closeness of the XRD and TEM sizes argues against polycrystalline aggregates. The shifted O–H and C=O bands in the FTIR spectrum point the same way as earlier reports: polyphenols and ellagitannins reduce $Ag^+$ and then stay on the surface as a capping layer [21, 22, 24]. The same organic shell explains why DLS gave a larger size and why the surface charge was negative [28]. The month-long stability is useful, because aggregated silver has less free surface and loses activity.

Antibacterial activity. MICs of 8–32 µg/mL are in the same range as those reported for other AgNPs, though particle size, capping and test methods differ so much between studies that close comparison is not really possible [7, 16, 36]. E. coli was the easiest to inhibit, and both S. aureus strains (methicillin-susceptible and MRSA) needed more silver. This fits the common finding that Gram-negative bacteria are more susceptible than Gram-positive ones, which is usually put down to differences in the cell envelope [9, 16]. The thick peptidoglycan layer of staphylococci probably slows the entry of particles and $Ag^+$, whereas the thin wall of E. coli

leaves its cytoplasmic membrane more open [8, 9]. K. pneumoniae was the exception. It is Gram-negative, yet it tolerated as much silver as MRSA, perhaps because its thick polysaccharide capsule, itself a major virulence factor, keeps the particles away from the cell surface [37]. An MBC/MIC ratio of 2 for every isolate means the particles kill rather than merely inhibit [38]. The time-kill data agree and add a time scale: 8 h for a 3-log fall in E. coli at 2× MIC, 12 h for MRSA. Faster killing at the higher dose is what one would expect from an agent with several targets: more silver means more $Ag^+$ and more ROS, so damage builds up sooner [10–13].

Activity against multidrug-resistant isolates. From a clinical point of view, what matters most is that ESBL-producing E. coli, MRSA and carbapenem-resistant K. pneumoniae were all still killed. In addition, AgNP zones exceeded gentamicin zones for each of the four MDR isolates. Earlier work has likewise found no cross-resistance between silver and standard antibiotics [17], which is understandable given their distinct modes of action: mechanisms such as β-lactamase production or target mutation shield one cellular target, whereas silver attacks the membrane, key enzymes and DNA at the same time [10, 12]. Silver resistance can still arise with repeated exposure [18]; finding out whether these isolates adapt would require serial passage at sub-MIC levels, which we did not carry out.

Cytotoxicity and selectivity. Silver is toxic to mammalian cells too; AgNPs have been shown to cause oxidative stress, mitochondrial damage and DNA strand breaks [39, 40]. Here, at least 87% of Vero cells survived at MIC-range concentrations, and the $IC_{50}$ exceeded the MICs by a factor of 3.5–14. The selectivity index for E. coli (SI > 10) implies a reasonable safety margin. For MRSA and K. pneumoniae, however, the margin was narrow: SI was 3.5 when calculated from the MIC and approximately 1.8 when calculated from the MBC. For these two organisms, topical use in dressings or surface coatings makes more sense than giving the particles systemically [5, 6]. We did not examine whether the plant-derived cap lowers cytotoxicity, and this remains an open question.

Limitations. We tested only one isolate of each species, so we cannot say how much susceptibility varies between strains. Toxicity was checked in a single non-human kidney line (Vero) and only at 24 h; human cells and longer exposures are needed before safety can be judged properly. We did not measure $Ag^+$ release or intracellular ROS, which means the mechanism discussed above is taken from the literature, not from our data. Gentamicin was also used at just one concentration and without MIC testing, so we cannot directly rank the particles against conventional antibiotics. Everything was done in vitro; there are no animal data yet, and agreed test standards for nanomaterials are still lacking [19].

## 5. Conclusion

Pomegranate peel extract yielded stable, crystalline AgNPs (mean core 22.5 nm) carrying a phenolic coat. All five clinical isolates were killed, MRSA, ESBL E. coli and carbapenem-resistant K. pneumoniae among them, with MICs of 8–32 µg/mL and MBCs of 16–64 µg/mL. Twice the MIC brought a 3-$\log_{10}$ fall within 8–12 h, while at least 87% of Vero cells survived at MIC-level concentrations. Peel is normally thrown away, which makes this a cheap source of antibacterial silver. More isolates, mechanistic and resistance studies, and animal work are the obvious next steps.

### *5.1 Declarations*

Ethics approval: Isolates were de-identified leftovers from routine diagnostic work; no patient data were accessed. The College of Medicine Scientific and Ethics Committee, University of Thi-Qar, approved the protocol.

Author contributions (CRediT): Ferial Y. Nazal: Conceptualization, Methodology, Investigation, Formal analysis, Visualization, Writing – original draft, Writing – review & editing. The author read and approved the final manuscript.

Data availability: Spectra, diffraction and FTIR files, TEM images, plate readings and colony counts will be shared by the author if asked.

**Funding:** This research received no external funding.

**Conflicts of Interest:** The authors declare no conflict of interest.

**Publisher's Note:** All claims expressed in this article are solely those of the authors and do not necessarily represent those of their affiliated organizations, or those of the publisher, the editors and the reviewers.

## References

[1] Antimicrobial Resistance Collaborators. Global burden of bacterial antimicrobial resistance in 2019: a systematic analysis. Lancet. 2022;399(10325):629-55. https://doi.org/10.1016/S0140-6736(21)02724-0

[2] Tacconelli E, Carrara E, Savoldi A, Harbarth S, Mendelson M, Monnet DL, et al. Discovery, research, and development of new antibiotics: the WHO priority list of antibiotic-resistant bacteria and tuberculosis. Lancet Infect Dis. 2018;18(3):318-27. https://doi.org/10.1016/S1473-3099(17)30753-3

[3] World Health Organization. WHO bacterial priority pathogens list, 2024: bacterial pathogens of public health importance to guide research, development and strategies to prevent and control antimicrobial resistance. Geneva: World Health Organization; 2024. Available from: https://www.who.int/publications/i/item/9789240093461

[4] Rai M, Yadav A, Gade A. Silver nanoparticles as a new generation of antimicrobials. Biotechnol Adv. 2009;27(1):76-83. https://doi.org/10.1016/j.biotechadv.2008.09.002

[5] Burdușel AC, Gherasim O, Grumezescu AM, Mogoantă L, Ficai A, Andronescu E. Biomedical applications of silver nanoparticles: an up-to-date overview. Nanomaterials (Basel). 2018;8(9):681. https://doi.org/10.3390/nano8090681

[6] Lee SH, Jun BH. Silver nanoparticles: synthesis and application for nanomedicine. Int J Mol Sci. 2019;20(4):865. https://doi.org/10.3390/ijms20040865

[7] Franci G, Falanga A, Galdiero S, Palomba L, Rai M, Morelli G, et al. Silver nanoparticles as potential antibacterial agents. Molecules. 2015;20(5):8856-74. https://doi.org/10.3390/molecules20058856

[8] Morones JR, Elechiguerra JL, Camacho A, Holt K, Kouri JB, Ramírez JT, et al. The bactericidal effect of silver nanoparticles. Nanotechnology. 2005;16(10):2346-53. https://doi.org/10.1088/0957-4484/16/10/059

[9] Sondi I, Salopek-Sondi B. Silver nanoparticles as antimicrobial agent: a case study on E. coli as a model for Gram-negative bacteria. J Colloid Interface Sci. 2004;275(1):177-82. https://doi.org/10.1016/j.jcis.2004.02.012

[10] Dakal TC, Kumar A, Majumdar RS, Yadav V. Mechanistic basis of antimicrobial actions of silver nanoparticles. Front Microbiol. 2016;7:1831. https://doi.org/10.3389/fmicb.2016.01831

[11] Le Ouay B, Stellacci F. Antibacterial activity of silver nanoparticles: a surface science insight. Nano Today. 2015;10(3):339-54. https://doi.org/10.1016/j.nantod.2015.04.002

[12] Durán N, Durán M, de Jesus MB, Seabra AB, Fávaro WJ, Nakazato G. Silver nanoparticles: a new view on mechanistic aspects on antimicrobial activity. Nanomedicine. 2016;12(3):789-99. https://doi.org/10.1016/j.nano.2015.11.016

[13] Xiu ZM, Zhang QB, Puppala HL, Colvin VL, Alvarez PJ. Negligible particle-specific antibacterial activity of silver nanoparticles. Nano Lett. 2012;12(8):4271-5. https://doi.org/10.1021/nl301934w

[14] Pal S, Tak YK, Song JM. Does the antibacterial activity of silver nanoparticles depend on the shape of the nanoparticle? A study of the Gram-negative bacterium Escherichia coli. Appl Environ Microbiol. 2007;73(6):1712-20. https://doi.org/10.1128/AEM.02218-06

[15] Agnihotri S, Mukherji S, Mukherji S. Size-controlled silver nanoparticles synthesized over the range 5-100 nm using the same protocol and their antibacterial efficacy. RSC Adv. 2014;4(8):3974-83. https://doi.org/10.1039/C3RA44507K

[16] Kim JS, Kuk E, Yu KN, Kim JH, Park SJ, Lee HJ, et al. Antimicrobial effects of silver nanoparticles. Nanomedicine. 2007;3(1):95-101. https://doi.org/10.1016/j.nano.2006.12.001

[17] Lara HH, Ayala-Núñez NV, Ixtepan-Turrent L, Rodríguez-Padilla C. Bactericidal effect of silver nanoparticles against multidrug-resistant bacteria. World J Microbiol Biotechnol. 2010;26(4):615-21. https://doi.org/10.1007/s11274-009-0211-3

[18] Panáček A, Kvítek L, Smékalová M, Večeřová R, Kolář M, Röderová M, et al. Bacterial resistance to silver nanoparticles and how to overcome it. Nat Nanotechnol. 2018;13(1):65-71. https://doi.org/10.1038/s41565-017-0013-y

[19] Rizzello L, Pompa PP. Nanosilver-based antibacterial drugs and devices: mechanisms, methodological drawbacks, and guidelines. Chem Soc Rev. 2014;43(5):1501-18. https://doi.org/10.1039/C3CS60218D

[20] Iravani S, Korbekandi H, Mirmohammadsadeghi SV, Zolfaghari B. Synthesis of silver nanoparticles: chemical, physical and biological methods. Res Pharm Sci. 2014;9(6):385-406. Available from: https://pmc.ncbi.nlm.nih.gov/articles/PMC4326978/

[21] Ahmed S, Ahmad M, Swami BL, Ikram S. A review on plants extract mediated synthesis of silver nanoparticles for antimicrobial applications: a green expertise. J Adv Res. 2016;7(1):17-28. https://doi.org/10.1016/j.jare.2015.02.007

[22] Singh P, Kim YJ, Zhang D, Yang DC. Biological synthesis of nanoparticles from plants and microorganisms. Trends Biotechnol. 2016;34(7):588-99. https://doi.org/10.1016/j.tibtech.2016.02.006

[23] Shankar SS, Rai A, Ahmad A, Sastry M. Rapid synthesis of Au, Ag, and bimetallic Au core-Ag shell nanoparticles using Neem (Azadirachta indica) leaf broth. J Colloid Interface Sci. 2004;275(2):496-502. https://doi.org/10.1016/j.jcis.2004.03.003

[24] Akhtar S, Ismail T, Fraternale D, Sestili P. Pomegranate peel and peel extracts: chemistry and food features. Food Chem. 2015;174:417-25. https://doi.org/10.1016/j.foodchem.2014.11.035

[25] Edison TJ, Sethuraman MG. Biogenic robust synthesis of silver nanoparticles using Punica granatum peel and its application as a green catalyst for the reduction of an anthropogenic pollutant 4-nitrophenol. Spectrochim Acta A Mol Biomol Spectrosc. 2013;104:262-4. https://doi.org/10.1016/j.saa.2012.11.084

[26] Mulvaney P. Surface plasmon spectroscopy of nanosized metal particles. Langmuir. 1996;12(3):788-800. https://doi.org/10.1021/la9502711

[27] Patterson AL. The Scherrer formula for X-ray particle size determination. Phys Rev. 1939;56(10):978-82. https://doi.org/10.1103/PhysRev.56.978

[28] Bhattacharjee S. DLS and zeta potential - what they are and what they are not? J Control Release. 2016;235:337-51. https://doi.org/10.1016/j.jconrel.2016.06.017

[29] Danaei M, Dehghankhold M, Ataei S, Hasanzadeh Davarani F, Javanmard R, Dokhani A, et al. Impact of particle size and polydispersity index on the clinical applications of lipidic nanocarrier systems. Pharmaceutics. 2018;10(2):57. https://doi.org/10.3390/pharmaceutics10020057

[30] Magiorakos AP, Srinivasan A, Carey RB, Carmeli Y, Falagas ME, Giske CG, et al. Multidrug-resistant, extensively drug-resistant and pandrug-resistant bacteria: an international expert proposal for interim standard definitions for acquired resistance. Clin Microbiol Infect. 2012;18(3):268-81. https://doi.org/10.1111/j.1469-0691.2011.03570.x

[31] Balouiri M, Sadiki M, Ibnsouda SK. Methods for in vitro evaluating antimicrobial activity: a review. J Pharm Anal. 2016;6(2):71-9. https://doi.org/10.1016/j.jpha.2015.11.005

[32] Clinical and Laboratory Standards Institute. Methods for dilution antimicrobial susceptibility tests for bacteria that grow aerobically. 11th ed. CLSI standard M07. Wayne (PA): CLSI; 2018.

[33] Wiegand I, Hilpert K, Hancock RE. Agar and broth dilution methods to determine the minimal inhibitory concentration (MIC) of antimicrobial substances. Nat Protoc. 2008;3(2):163-75. https://doi.org/10.1038/nprot.2007.521

[34] National Committee for Clinical Laboratory Standards. Methods for determining bactericidal activity of antimicrobial agents; approved guideline. NCCLS document M26-A. Wayne (PA): NCCLS; 1999.

[35] Mosmann T. Rapid colorimetric assay for cellular growth and survival: application to proliferation and cytotoxicity assays. J Immunol Methods. 1983;65(1-2):55-63. https://doi.org/10.1016/0022-1759(83)90303-4

[36] Panáček A, Kvítek L, Prucek R, Kolář M, Večeřová R, Pizurová N, et al. Silver colloid nanoparticles: synthesis, characterization, and their antibacterial activity. J Phys Chem B. 2006;110(33):16248-53. https://doi.org/10.1021/jp063826h

[37] Paczosa MK, Mecsas J. Klebsiella pneumoniae: going on the offense with a strong defense. Microbiol Mol Biol Rev. 2016;80(3):629-61. https://doi.org/10.1128/MMBR.00078-15

[38] Pankey GA, Sabath LD. Clinical relevance of bacteriostatic versus bactericidal mechanisms of action in the treatment of Gram-positive bacterial infections. Clin Infect Dis. 2004;38(6):864-70. https://doi.org/10.1086/381972

[39] AshaRani PV, Low Kah Mun G, Hande MP, Valiyaveettil S. Cytotoxicity and genotoxicity of silver nanoparticles in human cells. ACS Nano. 2009;3(2):279-90. https://doi.org/10.1021/nn800596w

[40] Vazquez-Muñoz R, Borrego B, Juárez-Moreno K, García-García M, Mota Morales JD, Bogdanchikova N, et al. Toxicity of silver nanoparticles in biological systems: does the complexity of biological systems matter? Toxicol Lett. 2017;276:11-20. https://doi.org/10.1016/j.toxlet.2017.05.007